DESIGN AND OPTIMIZATION OF LOW RCS PATCH ANTENNAS BASED ON A GENETIC ALGORITHM

X. Zhu, W. Shao*, J.-L. Li, and Y. Dong

School of Physical Electronics, University of Electronic Science and Technology of China (UESTC), Chengdu 610054, China

Abstract—In this article, a genetic algorithm (GA) is employed to the design of low radar cross section (RCS) patch antennas. Combined with the high frequency simulation software (HFSS) for antenna simulations, the GA performs the optimization of geometric parameters. In order to reduce the RCS while holding the satisfying radiation performance of antennas, the radiation model and scattering model are respectively calculated. The combination of proportionate selection and elitist model for the selection strategy is used to speed up the convergence of the GA. Two-point crossover is adopted to accelerate the converging speed and results in more fit individuals. Moreover, the whole design procedure is auto-controlled by programming the VBScript in the HFSS. Two examples of low RCS slot antennas are provided to verify the accuracy and efficiency of the proposed method.

1. INTRODUCTION

An antenna, which acts as a strong electromagnetic scatterer, is often the main contributor to the overall radar cross section (RCS) of a stealth aircraft [1–5]. Because of the basic radiation function of an antenna, the shaping method is one of the most effective methods for antenna RCS reduction [6]. In [7], circle and rectangular slots on the antenna patch cut off surface currents of high-order modes. [4, 8] introduce some types of fractal slots on an antenna patch to obtain the low backscattering. Frequency selective surface (FSS) structures are also presented to reduce RCS of reflect-array antennas [9, 10]. Lumped resistances which are soldered between the patches of mushroom-like high-impedance surface (HIGP) lead to a significant reduction

of the RCS of waveguide slot antennas [11]. The reduction of RCS in a wide frequency bandwidth is achievable by using dispersive metamaterials [12]. However, those parameters are difficult to get due to the simultaneous consideration on antenna radiation and scattering.

In view of the complexity of the low RCS antenna design, antenna geometric parameters are optimized with the differential evolution algorithm (DEA) to realize the RCS reduction [13]. Based on the separate DEA optimization for radiation and scattering, the individuals of bad radiation performance avoid the unnecessary RCS simulation of the method of moment (MoM). However, the final fitness calculations for each generation involve both of the radiation and scattering factors, which maybe lead to an inefficient solution.

Genetic algorithm (GA) optimizers are robust and stochastic search methods modeled on the principles and concepts of nature selection and evolution. The GA has been widely used for solving complex electromagnetic (EM) problems [14–17]. Varied antennas, such as monopole antennas [18, 19], Yagi antennas [20, 21], patch antennas [22–25] and array antennas [26–29] are designed for certain kinds of radiating target by GA optimization.

In this article, the lower RCS patch antennas are designed and optimized by combining the GA with a finite element method (FEM) based tool (high frequency simulation software, HFSS). The GA and HFSS are responsible for the optimization and simulation of low RCS antennas, respectively. An auto-controlled calculation is programmed based on the VBScript language in HFSS.

For rectangular patch antennas, the location and size of slots are optimized to obtain satisfying radiation and scattering performances. When applying the GA to low RCS antenna design, it is frequently necessary to solve EM problems with FEM-based HFSS hundreds of times, until the solution converges to a global extremum. In general, the EM simulations for antennas can be time consuming. Therefore, the amount of computation for each call of the EM solver by the GA needs to be reduced. The fitness value is calculated separately for the radiation and scattering targets in order to speed up the convergence. The combination of proportionate selection and elitist model as the selection strategy not only accelerates the converging speed but also keeps the global research. For the crossover strategy, the two-point crossover is utilized to hold the important generation modes effectively.

2. GA OPTIMIZATION FOR LOW RCS ANTENNAS

The flowchart of the whole calculation for low RCS antenna design is depicted in Fig. 1, which is made up of the optimization module

and simulation module. The GA program is the main body of the whole calculation, which obtains optimized geometry parameters of next generation and controls HFSS with VBScript by sending HFSS these parameters. With the VBScript, HFSS returns its results to the GA for calculating the fitnesses after finishing the simulation of the present generation. The two processes are being run alternately until the program is terminated or an optimal solution is obtained.

Initiation in the GA in Fig. 1 consists of filling an initial population with a predetermined number of randomly created chromosomes. Each of these chromosomes represents an individual prototype corresponding to an antenna structure. The GA sends antenna geometry parameters of the current generation to HFSS through the VBScript. Firstly, the antenna radiation models are established and simulated in HFSS. If an individual antenna meets the radiation requirements, such as S_{11} and gain conditions, it will be kept for the next scattering calculation. Otherwise, its fitness value is set to a large number and the scattering simulation for this individual antenna is skipped. Thus, a waste of time to simulate scattering models of the worse individuals is avoided. Secondly, only the individuals, whose radiation performances meet the predetermined requirements, continue to be simulated in HFSS to get their scattering performances. Based on the RCS results, the fitness of each individual of the current generation is calculated and transferred
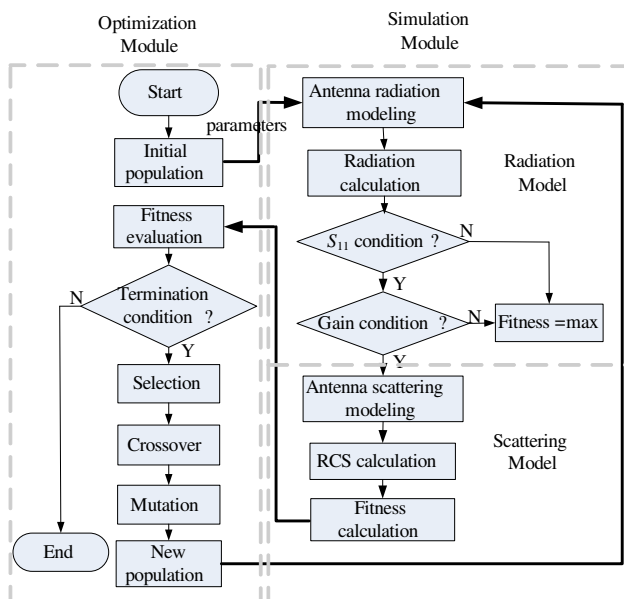

Figure 1. Flowchart of the calculation for low RCS antenna design.

to the GA. The fitness function is defined as follows:

$$fitness = \sum_{j=1}^{N} \left(\frac{1}{n} \sum_{i=1}^{n} A_{RCS(i)} \right) \qquad (1)$$

where A_{RCS} is the RCS value of an individual antenna, n is the number of the RCS sample point versus frequencies, and N stands for the different incident angles.

Next, the GA will produce a new generation from the current generation. From the results of the fitness evaluation, the proportionate selection strategy decides the probability of selecting an individual from the population. To speed up the convergence of the GA, at the same time, a certain amount of best individuals are saved and inserted into the new generation directly in the elitist strategy. In reproduction, a pair of individuals is selected to act as parents for crossover. A two-point crossover is adopted to rearrange the genes for producing better combinations of genes, thereby resulting in more fit individuals. The two-point crossover operator can also speed up the convergence of the GA compared with the single-point crossover. In order to avoid sticking at local optima, mutation occurs with a low probability, of a value of 0.01 in this article. Then, the new population, included previous elitist individuals, is produced and sent to HFSS for simulation again. The simulation and optimization are run alternatively until the termination condition is satisfied.

3. TWO EXAMPLES OF LOW RCS ANTENNA DESIGN

Because the slot design can restrain surface currents of an antenna, cutting off the surface currents of high-order modes can change the scattering properties of the antenna. The slots patch antenna as the first example shown in Fig. 2 consists of a $38 \times 28 \, \text{mm}^2$ patch symmetrical about y-axis and a $54 \times 44 \, \text{mm}^2$ ground plane. And the substrate is $2 \, \text{mm}$-thick RT5880 whose relative permittivity is 2.2. A coaxial probe is located $7 \, \text{mm}$ from the center of the antenna along y-axis. The width of each rectangular slot on the ground plane is $1 \, \text{mm}$, and the location G_i $(i = 1, 2, 3, 4)$ and length l_i $(i = 1, 2, 3, 4)$ of each slot are needed to be optimized. The rectangular patch antenna without slots is used as a reference antenna with a patch of $40 \times 29 \, \text{mm}^2$ and a ground of $70 \times 60 \, \text{mm}^2$.

In this example, a population of 40 individuals and maximal iteration of 20 generations are utilized. The S_{11} and gain condition in Radiation Model in Fig. 1 is set as $f_{\text{operating}} \in (3 \, \text{GHz}, 3.5 \, \text{GHz})$ and $gain > 7$, respectively. The best 10% individuals have been saved and inserted into the new population. Fig. 3 shows the average and
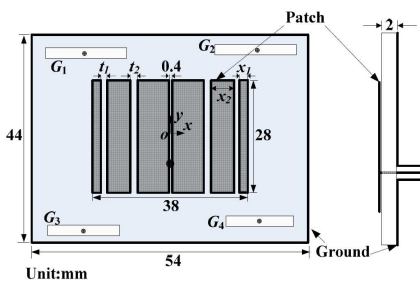
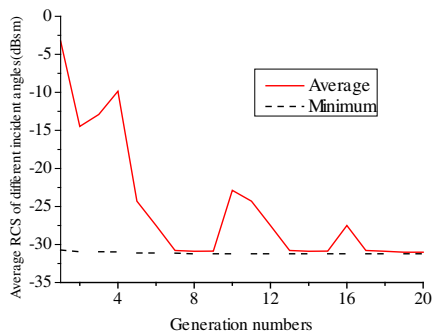**Figure 2.** Geometric structure of the slot patch antenna.

Figure 3. Convergence for RCS reduction of the GA program.

Table 1. Geometry of the optimized slot antenna (unit: mm).

Patch	x_1	t_1	x_2	t_2
	1.40	0.60	5.20	0.90
Ground slots		Location (x, y)		l
	G_1	$(-16.60,\ 10.71)$		17.60
	G_2	$(15.40,\ 17.76)$		16.80
	G_3	$(-14.20,\ -18.47)$		19.20
	G_4	$(16.60,\ -10.71)$		17.60

minimum values of average RCS of different incident angles for each GA generation. The optimization results are listed in Table 1.

The photographs of the reference antenna and the proposed antenna are shown in Fig. 4. Fig. 5 shows the measured and simulated return loss of the reference patch antenna and the optimized slot antenna. It can be observed that the impedance bandwidth of the slot antenna almost equals to that of the reference antenna. The measured results have a good consistency with simulation ones. In addition, both the *xoz*-plane and *yoz*-plane radiation patterns of the antennas are shown in Fig. 6. The slot antenna has normal radiation performance compared with the reference antenna.

In scattering modeling, the incident plane wave is with the θ polarization. Fig. 7 depicts two typical angles' RCS of the antennas versus frequency. In Fig. 7(a), the monostatic RCS value of the optimized antenna is reduced almost in the whole frequency range of 2–8 GHz. Especially, the RCS reduction in the frequency band of
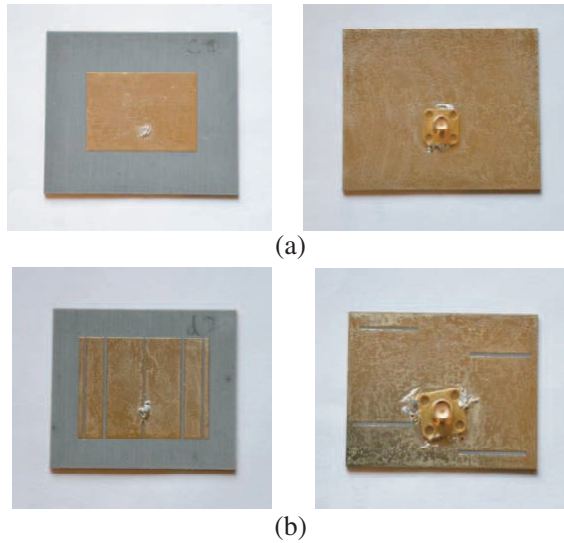
(a)

(b)

Figure 4. Photographs of the fabricated antennas with top and back views. (a) Reference antenna. (b) Slot antenna.
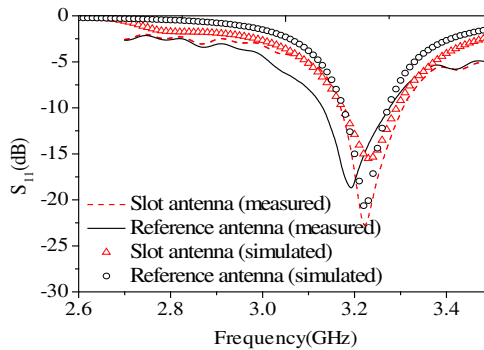

Figure 5. Return loss of the reference antenna and the slot antenna.

6–8 GHz is obvious for the incident angle of $\theta = 60°$ and $\varphi = 45°$. The average RCS of the optimized antenna and reference antenna in the whole frequency range are -31.49 dB and -26.71 dB, respectively. From Fig. 7(b), the RCS obtains 4–5 dB reduction between 4.5 and 6.5 GHz though the reduction of RCS is not obvious at low frequency. The average RCS of the optimized antenna and reference antenna in the whole frequency range are -31.32 dB and -27.44 dB, respectively.

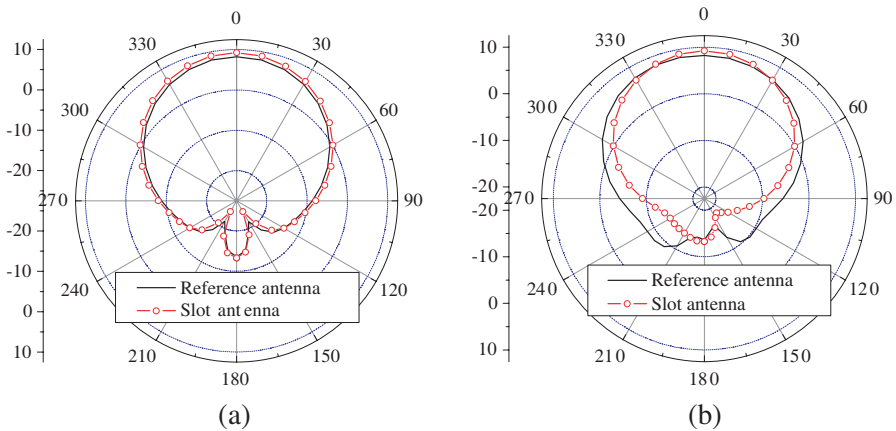In the second design example, the resonant frequency of the

Figure 6. Simulated radiation pattern of the reference antenna and the slot antenna at $3.23\,\mathrm{GHz}$. (a) xoz-plane. (b) yoz-plane.
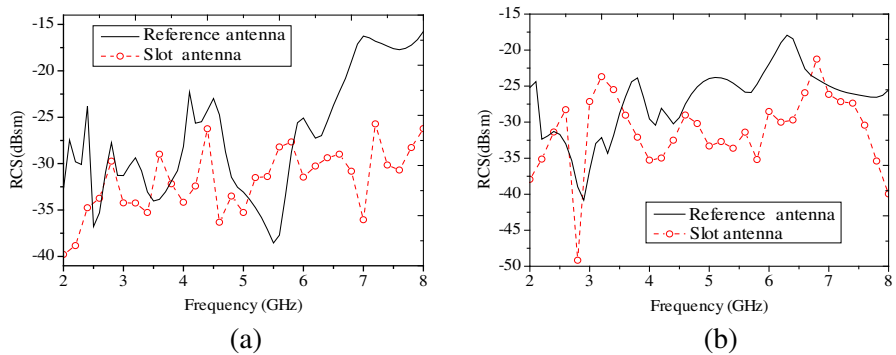

Figure 7. Simulated RCS of the reference antenna and the optimized slot antenna. (a) Incident angle ($\theta = 60°$, $\varphi = 45°$). (b) Incident angle ($\theta = 60°$, $\varphi = 90°$).

reference antenna is $2.66\,\mathrm{GHz}$. And its sizes of the patch and ground plane are $46 \times 35.5\,\mathrm{mm}^2$ and $80 \times 70\,\mathrm{mm}^2$, respectively. A slot patch antenna for the low RCS performance consists of a $40 \times 32\,\mathrm{mm}^2$ patch and a $60 \times 52\,\mathrm{mm}^2$ ground plane, shown in Fig. 8. A coaxial probe is located $7\,\mathrm{mm}$ from the center of the antenna along y-axis. The width of each rectangular slot on the patch is $2\,\mathrm{mm}$. And the location P_i ($i = 1, 2, 3, 4$), radius r_m ($m = 1, 2$) and length l_n ($n = 3, 4$) of each slot are variables. The width of each rectangular slot on the ground plane is $1\,\mathrm{mm}$, and the location G_i ($i = 1, 2, 3, 4$) and length l_i ($i = 1, 2, 3, 4$) of each slot are needed to be optimized. Two antenna's substrates are
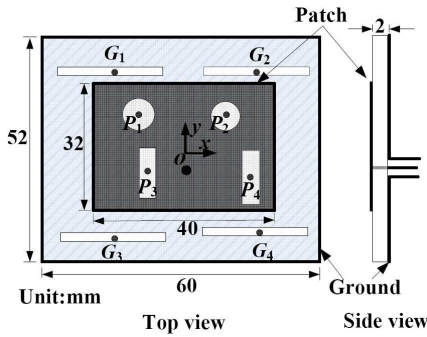
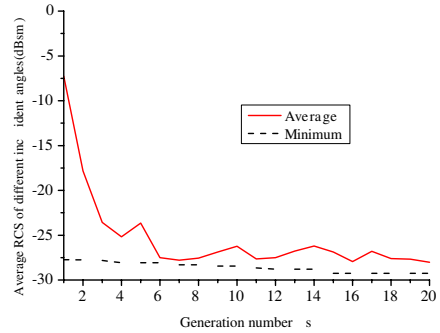**Figure 8.** Geometry structure of the slot patch antenna.

Figure 9. Convergence for RCS reduction of the GA program.

Table 2. Geometry of the optimized slot antenna (unit: mm).

	Patch slots			Ground slots	
	Location (x, y)	r or l		Location (x, y)	l
P_1	$(-8.00, 7.33)$	$r = 5.33$	G_1	$(-18.60, 13.55)$	16.56
P_2	$(8.00, 7.67)$	$r = 5.67$	G_2	$(18.50, 5.98)$	19.67
P_3	$(-8.53, -10.00)$	$l = 8.44$	G_3	$(14.67, -20.32)$	17.33
P_4	$(14.67, -20.32)$	$l = 8.44$	G_4	$(19.27, -9.17)$	18.11

the same as those in first example.

In this example, a population of 40 individuals and maximal iteration of 20 generations are adopted, too. Similarly, the S_{11} condition and gain condition in Radiation Model is set as $f_{\text{operating}} \in$ (2.5 GHz, 2.8 GHz) and $gain > 7$, respectively. The best 10% individuals are saved and inserted into the new population. The average and minimum values of average RCS of different incident angles for each GA generation are shown in Fig. 9. The optimization results are given in Table 2.

The photographs of the reference antenna and slot antenna are shown in Fig. 10. Fig. 11 depicts the measured and simulated impedance bandwidths of the two antennas. The relative error of 3% between simulation and measurement is mostly due to the influence of the stability of the substrate processing and etching precision. In addition, the *xoz*-plane and the *yoz*-plane radiation patterns of antennas are shown in Fig. 12. The slot antenna has normal radiation performance compared with that of the reference antenna.
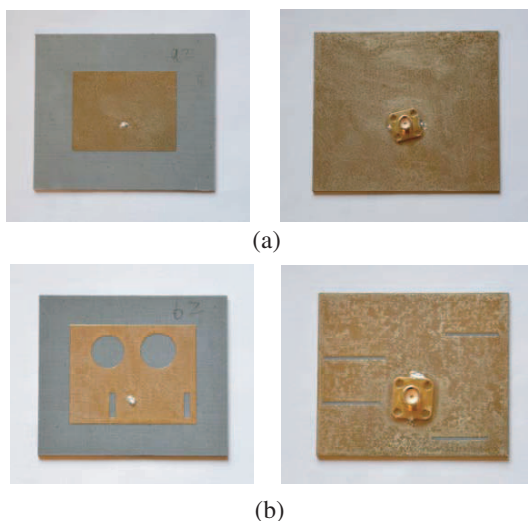
(a)

(b)

Figure 10. Photographs of the fabricated antennas with top and back views. (a) Reference antenna. (b) Slot antenna.
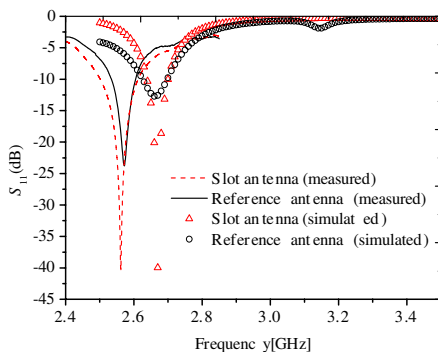

Figure 11. Return loss of the reference antenna and the optimized slot antenna.

In this example, the incident wave is also the θ-polarized plane wave. Fig. 13 shows the monostatic RCS of the two antennas versus frequency at two typical incident angles. Compared to the reference antenna, the RCS value of the optimized slot antenna is reduced distinctly in the whole frequency range of 2–8 GHz. For example, the average RCS of the optimized antenna and reference antenna in the whole frequency range of 2–8 GHz are -30.89 dB and -26.23 dB, respectively, for the incident angle of $\theta = 60°$ and $\varphi = 45°$.
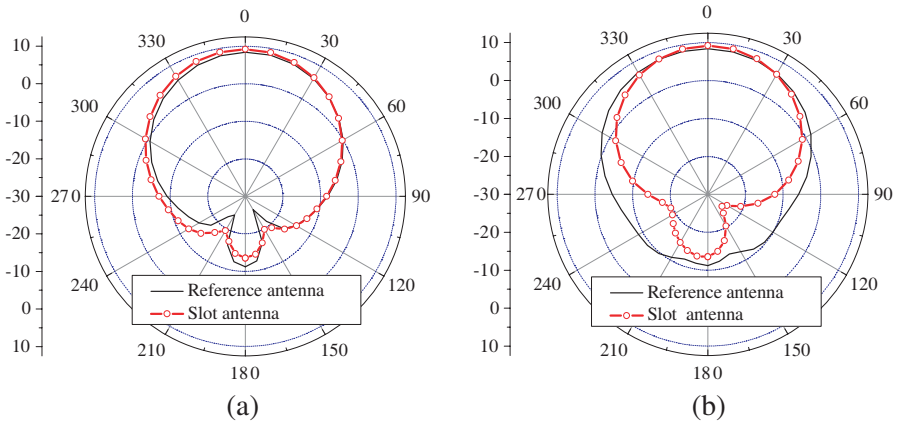
Figure 12. Simulated radiation patterns of the reference antenna and the slot antenna at 2.66 GHz. (a) *xoz*-plane. (b) *yoz*-plane.

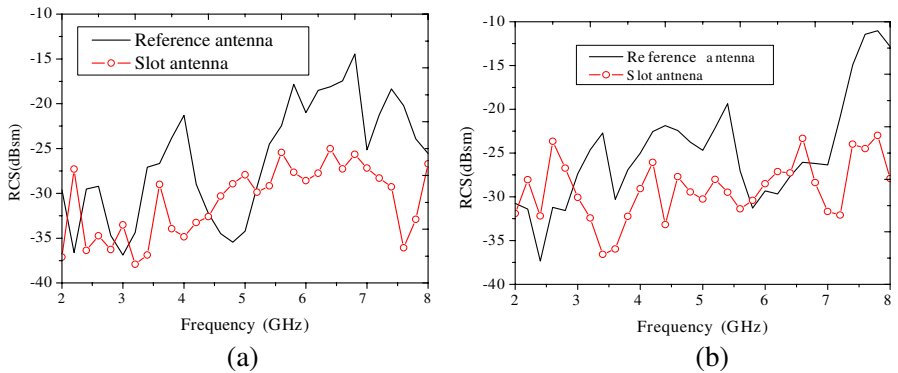**Figure 13.** Simulated RCS of the reference antenna and the optimized slot antenna. (a) Incident angle ($\theta = 60°$, $\varphi = 45°$). (b) Incident angle ($\theta = 60°$, $\varphi = 90°$).

4. CONCLUSION

An efficient method, which combines the GA optimizer with HFSS to design low RCS patch antennas, has been presented in this article. The proportionate selection together with the elitist model for the selection strategy and the two-point crossover is used to speed up the convergence of the GA. Only the individuals meeting the radiation requirement will be simulated in the scattering model, and values of fitness merely consider the scattering performance of the individuals. And VBScript in HFSS realizes the data exchange between the

optimization module and simulation module automatically. Two examples of patch antennas are designed with the proposed method. The simulated and measured results show that the optimized slot antennas realize the RCS reduction in a broad frequency range of 2–8 GHz at different incident angles, while maintaining good radiation performances.

ACKNOWLEDGMENT

REFERENCES

1. Jiang, W., T. Hong, Y. Liu, S.-X. Gong, Y. Guan, and S. Cui, "A novel technique for radar cross section reduction of printed antennas," *Journal of Electromagnetic Waves and Applications*, Vol. 24, No. 1, 51–60, 2010.

2. Hong, T., L.-T. Jiang, Y.-X. Xu, S.-X. Gong, and W. Jiang, "Radiation and scattering analysis of a novel circularly polarized slot antenna," *Journal of Electromagnetic Waves and Applications*, Vol. 24, No. 13, 1709–1720, 2010.

3. Xu, H.-Y., H. Zhang, K. Lu, and X.-F. Zeng, "A holly-leaf-shaped monopole antenna with low RCS for UWB application," *Progress In Electromagnetics Research*, Vol. 117, 35–50, 2011.

4. Xu, H.-Y., H. Zhang, X. Yin, and K. Lu, "Ultra-wideband Koch fractal antenna with low backscttering cross section," *Journal of Electromagnetic Waves and Applications*, Vol. 24, No. 17–18, 2615–2623, 2010.

5. Gonzalez, C. G., Y. Alvarez Lopez, A. D. Casas, and F. Las-Heras Andres, "Characterization of antenna interaction with scatterers by means of equivalent currents," *Progress In Electromagnetics Research*, Vol. 116, 185–202, 2011.

6. Knot, E. F., J. F. Sbaeffer, and M. T. Tuley, *Radar Cross Section*, 2nd edition, Artech House, London, 1993.

7. Zhao, S.-C., B.-Z. Wang, and Q.-Q. He, "Broadband cross section reduction of a rectangular patch antenna," *Progress In Electromagnetics Research*, Vol. 79, 263–275, 2008.

8. Kumar, R. and P. Malathi, "Design of CPW-fed ultra wideband fractal antenna and backscattering reduction," *Journal of*

Microwaves, Optoelectronics and Electromagnetic Applications, Vol. 9, No. 1, 10–19, 2010.

9. Misran, N., R. Cahill, and V. F. Fusco, "RCS reduction technique for reflectarray antennas," *Electronics Letters*, Vol. 39, No. 23, 1630–1632, 2003.

10. Ren, L.-S., Y.-C. Jiao, J.-J. Zhao, and F. Li, "RCS reduction for a FSS-backed reflectarray using a ring element," *Progress In Electromagnetics Research Letters*, Vol. 26, 115–123, 2011.

11. Zheng, Q.-R., Y.-M. Yan, X.-Y. Cao, and N.-C. Yuan, "High impedance ground plane (HIGP) incorporated with resistance for radar cross section (RCS) reduction of antenna," *Progress In Electromagnetics Research*, Vol. 84, 307–319, 2008.

12. Oraizi, H. and A. Abdolali, "Combination of MLS, GA & CG for the reduction of RCS of multilayered cylindrical structures composed of dispersive metamaterials," *Progress In Electromagnetics Research B*, Vol. 3, 227–253, 2008.

13. Wang, W., S. Gong, X. Wang, Y. Guan, and W. Jiang, "Differential evolution algorithm and method of moments for the design of low-RCS antenna," *IEEE Antennas and Wireless Propagation Letters*, Vol. 9, 295–298, 2010.

14. Rahmat-Samii, Y. and E. Michielssen, *Electromagnetic optimization by Genetic Algorithms*, John Wiley & Sons, New York, 1999.

15. Xu, O., "Collimation lens design using AI-GA technique for Gaussian radiators with arbitrary aperture field distribution," *Journal of Electromagnetic Waves and Applications*, Vol. 25, No. 5–6, 743–754, 2011.

16. Jian, L., G. Xu, J. Song, H. Xue, D. Zhao, and J. Liang, "Optimum design for improving modulating-effect of coaxial magnetic gear using response surface methodology and genetic algorithm," *Progress In Electromagnetics Research*, Vol. 116, 297–312, 2011.

17. Reza, A. W., M. S. Sarker, and K. Dimyati, "A novel integrated mathematical approach of ray-tracing and genetic algorithm for optimizing indoor wireless coverage," *Progress In Electromagnetics Research*, Vol. 110, 147–162, 2010.

18. Kerkhoff, A. J., R. L. Rogers, and H. Ling, "Design and analysis of planar monopole antennas using a genetic algorithm approach," *IEEE Transactions on Antennas and Propagation*, Vol. 52, No. 10, 2709–2718, 2004.

19. Kerkhoff, A. J. and H. Ling, "Design of a band-notched planar monopole antenna using genetic algorithm optimization," *IEEE*

Transactions on Antennas and Propagation, Vol. 55, No. 3, 604–610, 2007.

20. Jones, E. A. and W. T. Joines, "Design of Yagi-Uda antennas using genetic algorithms," *IEEE Transactions on Antennas and Propagation*, Vol. 45, No. 9, 1386–1392, 1997.

21. Kuwahara, Y., "Multiobjective optimization design of Yagi-Uda antenna," *IEEE Transactions on Antennas and Propagation*, Vol. 53, No. 6, 1984–1992, 2005.

22. Villegas, F. J., T. Cwik, Y. Rahmat-Samii, and M. Manteghi, "A parallel electromagnetic genetic algorithm optimization (EGO) application for patch antenna design," *IEEE Transactions on Antennas and Propagation*, Vol. 52, No. 9, 2424–2435, 2004.

23. Pu, T., K.-M. Huang, B. Wang, and Y. Yang, "Application of micro-genetic algorithm to the design of matched high gain patch antenna with zero-refractive-index matematerial lens," *Journal of Electromagnetic Waves and Applications*, Vol. 24, No. 8–9, 1207–1217, 2010.

24. Zhang, Y.-J., S.-X. Gong, X. Wang, and W.-T. Wang, "A hybrid genetic-algorithm space-mapping method for the optimization of broadband aperture-coupled asymmetrical U-shaped slot antennas," *Journal of Electromagnetic Waves and Applications*, Vol. 24, No. 16, 2139–2153, 2010.

25. Dadgarnia, A. and A. A. Heidari, "A fast systematic approach for microstrip antenna design and optimization using ANFIS and GA," *Journal of Electromagnetic Waves and Applications*, Vol. 24, No. 16, 2207–2221, 2010.

26. Allard, R. J., D. H. Werner, and P. L. Werner, "Radiation pattern synthesis for arrays of conformal antennas mounted on arbitrarily-shaped three-dimensional platforms using genetic algorithms," *IEEE Transactions on Antennas and Propagation*, Vol. 51, No. 5, 1054–1062, 2003.

27. Villegas, F. J., "Parallel genetic-algorithm optimization of shaped beam coverage areas using planar 2-D phased arrays," *IEEE Transactions on Antennas and Propagation*, Vol. 55, No. 6, 1745–1753, 2007.

28. Jain, R. and G. S. Mani, "Dynamic thinning of antenna array using genetic algorithm," *Progress In Electromagnetics Research B*, Vol. 32, 1–20, 2011.

29. Siakavara, K., "Novel fractal antenna arrays for satellite networks: Circular ring Sierpinski carpet arrays optimized by genetic algorithms," *Progress In Electromagnetics Research*, Vol. 103, 115–138, 2010.